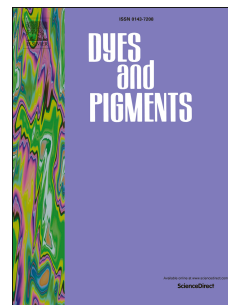


Accepted Manuscript

Development of naphthalimide-functionalized thermochromic conjugated polydiacetylenes and their reversible green-to-red chromatic transition in the solid state

Naveen Mergu, Hyorim Kim, Gisu Heo, Young-A. Son



PII: S0143-7208(19)30033-6

DOI: <https://doi.org/10.1016/j.dyepig.2019.01.058>

Reference: DYPI 7331

To appear in: *Dyes and Pigments*

Received Date: 5 January 2019

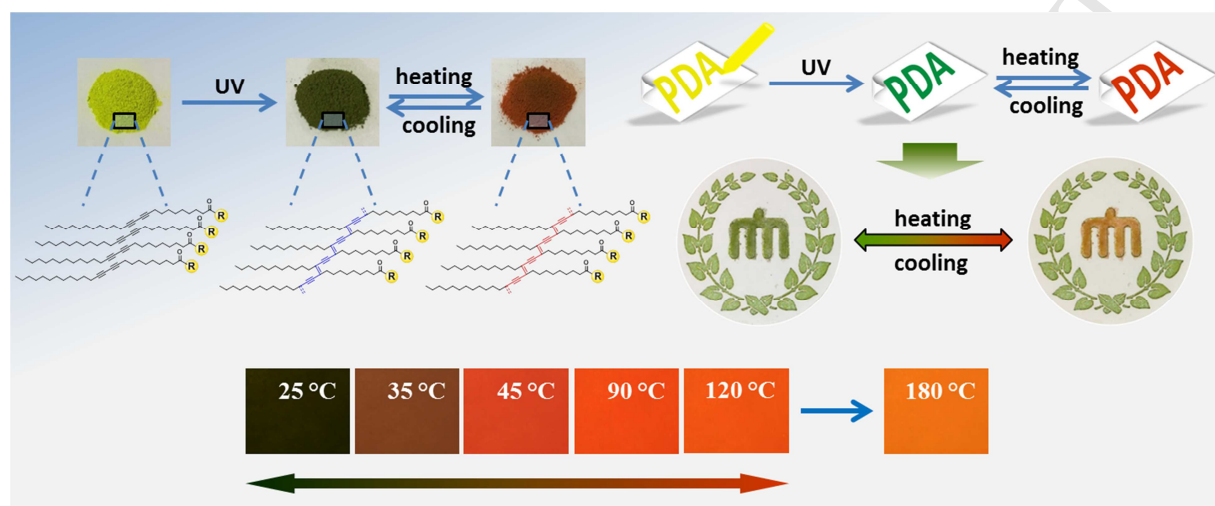
Revised Date: 28 January 2019

Accepted Date: 30 January 2019

Please cite this article as: Mergu N, Kim H, Heo G, Son Y-A, Development of naphthalimide-functionalized thermochromic conjugated polydiacetylenes and their reversible green-to-red chromatic transition in the solid state, *Dyes and Pigments* (2019), doi: <https://doi.org/10.1016/j.dyepig.2019.01.058>.

This is a PDF file of an unedited manuscript that has been accepted for publication. As a service to our customers we are providing this early version of the manuscript. The manuscript will undergo copyediting, typesetting, and review of the resulting proof before it is published in its final form. Please note that during the production process errors may be discovered which could affect the content, and all legal disclaimers that apply to the journal pertain.

Graphical abstract



1 **Development of naphthalimide-functionalized thermochromic**
2 **conjugated polydiacetylenes and their reversible green-to-red**
3 **chromatic transition in the solid state**

4
5 Naveen Mergu, Hyorim Kim, Gisu Heo, Young-A Son*

6
7 Department of Advanced Organic Materials Engineering, Chungnam National University, 220

8 Gung-dong, Yuseong-gu, Daejeon 305-764, South Korea

9
10
11
12
13
14
15
16
17
18
19
20
21
22
23

*Corresponding author. Tel.: +82 42 821 6620; Fax: +82 42 821 8870.

E-mail addresses: yason@cnu.ac.kr (Y.-A. Son).

24 **Abstract**

25 Development of PDAs has received great attention in many fields due to their optical and
26 chromatic properties towards external stimuli. In this article, two novel PDAs (**NPI-PDA1** and
27 **NPI-PDA2**) containing naphthalimide as a head group are designed and synthesized through
28 self-assembly followed by topochemical polymerization, and these compounds show a reversible
29 green-to-red colorimetric transition upon heating. PEO-embedded films are fabricated to
30 facilitate the investigation of the thermochromic properties, and the surface morphologies of the
31 films are observed by SEM analysis. The thermochromic behavior and color transitions are
32 observed using photography and electronic absorption spectroscopy. The changes in the
33 extended ene-yne conjugated system of the polymer during heat treatment are successfully
34 monitored by Raman spectrometry. Moreover, PDA-embedded crayon wax-based hand-writable
35 pens are fabricated and used efficiently on a solid substrate. **NPI-PDA1** and **NPI-PDA2** display
36 excellent reversibility in the temperature ranges of 25–120 °C and 25–160 °C, respectively in the
37 PEO polymer and paraffin wax matrices.

38

39 **Keywords:** Polydiacetylene, Thermochromism, Green-to-red color transition, PEO films,
40 Crayon pen

41

42 1. Introduction

43 Polydiacetylenes (PDAs) are important conjugated polymers that have alternating double
44 and triple bonds in the main polymer chain. PDAs are generally obtained by irradiation of self-
45 assembled diacetylene monomers with UV (254 nm) or γ -rays, and these reactions do not require
46 chemical initiators or catalysts nor are purification steps necessary to obtain pure PDAs. The
47 polymerization takes place because the spacing between the monomer alkyl chains is small and
48 similar to the spacing required for the diacetylene backbone to form and because of the
49 intramolecular interactions among the monomer's sidechains [1–6]. However, for polymerization
50 in the solid state, the diacetylene units must be properly oriented in relation to each other. A
51 distance of 4.9 Å between the two reactive carbon atoms and an angle of 45° relative to the
52 acetylene axis are required for this polymerization [7,8].

53 PDAs have received a substantial amount of attention since their discovery due to their
54 facile self-polymerization and their optical and chromic properties including the unique blue-to-
55 red and non-fluorescence to red-fluorescence transitions upon exposure to external stimuli such
56 as heat, solvent, pH changes, mechanical stress, electrical current and ligand-receptor interaction
57 [9–20]. The color change can easily be observed by the naked-eye. The color transformations of
58 PDAs are due to the π - π^* transition in the linear π -conjugated polymer backbone. The monomers
59 alone do not show an absorption band, but an absorption band appears at approximately 650 nm
60 upon polymerization. If the effective conjugation length is reduced due to strain or torsion
61 applied to the backbone, the absorption maximum shifts to approximately 550 nm, which
62 corresponds to a red color. These smart materials have been effectively used as temperature
63 sensors and to monitor various biologically, chemically and environmentally important analytes
64 [21–38]. To date, the majority of reported thermochromic PDAs show blue-to-red color changes

65 above room temperature (typically >40 °C). In the past few years, PDA-like conjugate polymers
66 have been important materials for developing advanced systems and devices in various fields due
67 to their intrinsic electronic, magnetic, photonic and spectroscopic properties [39–44].

68 To date, numerous PDAs were reported, which are mainly showing a reversible
69 thermochromic behavior with a one-way blue-to-red color transitions. Also, the PCDA
70 consisting of ethylene diamine was also reported, which showed blue-to-red color transition at
71 room temperature [45]. In previous reports, aza-substituted PCDA were used to achieve green-
72 colored PDAs; however, due to steric hindrance, some of these compounds could not be
73 polymerized, and some of those that did polymerize, produced regular blue-colored PDAs [46–
74 49]. A green-to-red color transition was achieved by a subtractive color mixing method (external
75 mixing) and reported recently by our research group [50]. From the knowledge of the color
76 theory, we have extended the strategy to obtain PDAs that shows direct green-to-red color
77 transition without mixing additional color. Recently, the development of directly writable
78 techniques for depositing functional materials on solid substrates has attracted great attention
79 [51–57]. In particular, pen-on-paper type approaches are very interesting since they enable the
80 preparation of diverse patterned images on solid substrates with the flexibility afforded by
81 drawing in an inexpensive manner [58].

82 In the present work, we have developed new PDAs (**NPI-PDA**) containing naphthalimide
83 as a head group by a condensation reaction using 10,12-pentacosadiynoic acid (PCDA) (see
84 **Figure S1** in the SI). This is the first example of a PDA with a reversible green-to-red color
85 transition at 45 °C instead of a blue-to-red transition, and the compound can return to its initial
86 color (green) when temperature is decreased. Furthermore, thermochromic color transitions

87 displayed by **NPI-PDA**-embedded PEO films are highly reversible and occur over a short
88 temperature range (25 to 45 °C).

89

90 **2. Experimental Section**

91 *2.1. Materials and Instruments*

92 4-Bromo-1,8-naphthalic anhydride, n-butylamine, anhydrous ethylenediamine, anhydrous
93 piperazine, N,N'-dicyclohexylcarbodiimide and 4-dimethylaminopyridine were purchased from
94 TCI. 10,12-Pentacosadiynoic acid (PCDA) was purchased from Sigma-Aldrich. All other
95 solvents were purchased from commercial sources and used without further purification. The ¹H
96 and ¹³C nuclear magnetic resonance (NMR) spectra were collected on a Bruker AVANCE III
97 spectrometer at 300 and 600 MHz, and CDCl₃ was used as the solvent. Mass spectra were
98 recorded on AB Sciex 4000 QTRAP and Bruker micrOTOF-Q mass spectrometers. Solid-state
99 absorption spectra were acquired on a SolidSpec-3700 diffuse reflectance UV-vis-NIR
100 spectrophotometer. UV-vis spectra of the PEO films were collected using a Shimadzu UV-2600
101 spectrophotometer. Thermogravimetric analysis (TGA) and differential scanning calorimetry
102 (DSC) were conducted on a Mettler-Toledo TGA/DSC1 thermal analyzer at a heating/cooling
103 rate of 10 °C/min in a nitrogen stream. SEM analysis for the polymer thin films was conducted
104 using a Zeiss MERLIN field emission scanning electron microscope. Raman spectra were
105 obtained on a Horiba Jobin Yovn LabRAM HR-800 Raman spectrometer with excitation at 785
106 nm laser under ambient conditions.

107

108 *2.2. Preparation of diacetylene*

109 **Synthesis of naphthalimide (A):** **A** was prepared according to the literature method [59]. **A**
110 mixture of 4-bromo-1,8-naphthalic anhydride (2.77 g, 10 mmol) and butylamine (0.88 g, 12
111 mmol) in ethanol (50 mL) was refluxed for 8 hours. Then, the reaction mixture was concentrated
112 under reduced pressure and purified by column chromatography using a mixture of hexane/DCM
113 (7:3) as the eluent. After drying under reduced pressure, the reaction yielded **A** as a white solid
114 (3.0 g, 90%). ^1H NMR (300 MHz, CDCl_3 , δ): 8.55 (dd, $J = 1.2, 7.2$ Hz, 1H; Ar H), 8.45 (dd, $J =$
115 1.2, 8.4 Hz, 1H; Ar H), 8.31 (d, $J = 8.1$ Hz, 1H; Ar H), 7.94 (d, $J = 7.8$ Hz, 1H; Ar H), 7.75 (t, J
116 = 7.2 Hz, 1H; Ar H), 4.09 (t, $J = 7.5$ Hz, 2H; CH_2), 1.69–1.59 (m, 2H, CH_2), 1.37 (sext, $J = 7.5$
117 Hz, 2H; CH_2), 0.90 (t, $J = 7.5$ Hz, 3H; CH_3); ^{13}C NMR (150 MHz, CDCl_3 , δ): 133.1, 131.9,
118 131.1, 131.0, 130.5, 130.1, 128.9, 128.0, 123.1, 122.2, 40.3, 30.1, 20.3, 13.8.

119 **Synthesis of naphthalimide derivative (B):** **A** (1.0 g, 3 mmol), ethylenediamine (1.8 g, 30
120 mmol), and piperazine (1.3 g, 15 mmol) were refluxed in ethanol (30 mL) for 72 hours. The
121 mixture was then concentrated and purified by column chromatography using DCM/MeOH
122 (90:10 for **B1** and 95:5 for **B2**) as the eluent, and **B** was isolated as a yellow solid (0.79 g, 84%
123 of **B1** and 0.89 g, 87% of **B2**).

124 **B1:** ^1H NMR (600 MHz, CDCl_3 , δ): 8.53 (d, $J = 7.2$ Hz, 1H; Ar H), 8.41 (d, $J = 8.4$ Hz, 1H; Ar
125 H), 8.15 (d, $J = 8.4$ Hz, 1H; Ar H), 7.57 (t, $J = 7.2$ Hz, 1H; Ar H), 6.65 (d, $J = 8.4$ Hz, 1H; Ar H),
126 6.19 (s, 1H, NH), 4.14 (t, $J = 7.8$ Hz, 2H; CH_2), 3.39 (q, $J = 6.0$ Hz, 2H; CH_2), 3.16 (t, $J = 6.0$ Hz
127 2H; CH_2), 1.72–1.67 (m, 2H, CH_2), 1.56 (s, 2H, NH_2), 1.42 (sext, $J = 7.8$ Hz, 2H; CH_2), 0.96 (t, J
128 = 7.8 Hz, 3H; CH_3); ^{13}C NMR (150 MHz, CDCl_3 , δ): 164.7, 164.1, 149.6, 134.4, 131.0, 129.7,
129 126.2, 124.6, 123.1, 120.4, 110.3, 104.4, 44.9, 40.2, 39.9, 30.3, 20.4, 13.8. ESI-MS m/z : [$\text{M} +$
130 $\text{H}]^+$ calcd for $\text{C}_{18}\text{H}_{21}\text{N}_3\text{O}_2$, 312.2; found, 312.3.

131 **B2**: ^1H NMR (600 MHz, CDCl_3 , δ): 8.57 (d, $J = 7.2$ Hz, 1H; Ar H), 8.51 (d, $J = 7.8$ Hz, 1H; Ar
132 H), 8.41 (d, $J = 8.4$ Hz, 1H; Ar H), 7.68 (t, $J = 7.8$ Hz, 1H; Ar H), 7.20 (d, $J = 7.8$ Hz, 1H; Ar H),
133 4.16 (t, $J = 7.2$ Hz, 2H; CH_2), 3.24–3.19 (m, 8H, CH_2), 1.70 (qn, $J = 7.8$ Hz, 2H; CH_2), 1.44
134 (sext, $J = 7.2$ Hz, 2H; CH_2), 1.24 (s, 1H, NH), 0.96 (t, $J = 7.2$ Hz, 3H; CH_3); ^{13}C NMR (150
135 MHz, CDCl_3 , δ): 164.5, 164.0, 156.3, 132.5, 131.20, 130.2, 129.9, 126.2, 125.6, 123.3, 116.8,
136 114.9, 54.4, 46.2, 40.1, 30.3, 20.4, 13.8. ESI-MS m/z : $[\text{M} + \text{H}]^+$ calcd for $\text{C}_{20}\text{H}_{23}\text{N}_3\text{O}_2$, 338.2;
137 found, 337.8.

138 **Synthesis of diacetylene monomers (NPI-DA)**: As shown in **Scheme 1**, a dichloromethane
139 (DCM) solution containing **B** (1.5 mmol), 10,12-pentacosadiynoic acid (PCDA) (0.56 g, 1.5
140 mmol), N,N' -dicyclohexylcarbodiimide (DCC) (0.5 g, 2.5 mmol) and 4-(dimethylamino)pyridine
141 (DMAP) (30 mg) was stirred overnight at room temperature. The mixture was concentrated
142 under reduced pressure and purified by column chromatography (DCM/MeOH; 99:1) to afford
143 **NPI-DA** as green-yellow solid (750 mg, 75% of **NPI-DA1** and 821 mg, 79% of **NPI-DA2**).

144 **NPI-DA1**: ^1H NMR (600 MHz, CDCl_3 , δ): 8.56 (d, $J = 7.2$ Hz, 1H; Ar H), 8.38 (d, $J = 7.8$ Hz,
145 1H; Ar H), 8.23 (d, $J = 8.4$ Hz, 1H; Ar H), 7.63 (t, $J = 7.2$ Hz, 1H; Ar H), 7.20 (s, 1H, NH), 6.48
146 (d, $J = 8.4$ Hz, 1H; Ar H), 6.37 (t, $J = 6.6$ Hz, 1H; NH), 4.15 (t, $J = 7.2$ Hz, 2H; CH_2), 3.76 (q, J
147 = 6.0 Hz, 2H; CH_2), 3.42 (q, $J = 4.2$ Hz, 2H, CH_2), 2.28 (t, $J = 7.2$ Hz, 2H; CH_2), 2.23 (t, $J = 7.2$
148 Hz, 2H; CH_2), 2.16 (t, $J = 7.2$ Hz, 2H; CH_2), 1.73–1.69 (m, 2H, CH_2), 1.67–1.63 (m, 2H, CH_2),
149 1.50 (qn, $J = 7.2$ Hz, 2H; CH_2), 1.46–1.38 (m, 4H, CH_2), 1.37–1.13 (m, 23H, CH_2), 1.15–1.08
150 (m, 3H, CH_2), 0.96 (t, $J = 7.2$ Hz, 3H; CH_3), 0.87 (t, $J = 7.2$ Hz, 3H; CH_3); ^{13}C NMR (150 MHz,
151 CDCl_3 , δ): 176.6, 164.8, 164.3, 150.1, 134.4, 131.1, 129.8, 127.2, 124.9, 122.8, 120.4, 109.9,
152 103.1, 77.6, 77.3, 65.4, 65.2, 46.7, 39.9, 38.9, 36.6, 33.9, 31.9, 30.3, 29.6, 29.6, 29.5, 29.4, 29.3,

153 29.1, 29.0, 28.9, 28.8, 28.8, 28.6, 28.4, 28.2, 25.7, 25.6, 24.9, 22.7, 20.4, 19.1, 14.1, 13.9. HRMS

154 m/z : $[M + Na]^+$ calcd for $C_{43}H_{61}N_3O_3$, 690.4611; found, 690.4600.

155 **NPI-DA2**: 1H NMR (600 MHz, $CDCl_3$, δ): 8.60 (dd, $J = 1.2, 7.2$ Hz, 1H; Ar H), 8.52 (d, $J = 7.8$

156 Hz, 1H; Ar H), 8.42 (dd, $J = 1.2, 8.4$ Hz, 1H; Ar H), 7.72 (t, $J = 7.2$ Hz, 1H; Ar H), 7.22 (d, $J =$

157 8.4 Hz, 1H; Ar H), 4.16 (t, $J = 7.2$ Hz, 2H; CH_2), 3.94 (s, 2H, CH_2), 3.79 (s, 2H, CH_2), 3.25–3.21

158 (m, 4H, CH_2), 2.24 (t, $J = 7.8$ Hz, 2H; CH_2), 2.23 (q, $J = 7.8$ Hz, 4H; CH_2), 1.73–1.65 (m, 4H,

159 CH_2), 1.50 (sext, $J = 7.2$ Hz, 4H; CH_2), 1.44 (q, $J = 7.2$ Hz, 2H; CH_2), 1.41–1.25 (m, 26H, CH_2),

160 0.97 (t, $J = 7.2$ Hz, 3H; CH_3), 0.87 (t, $J = 7.2$ Hz, 3H; CH_3); ^{13}C NMR (150 MHz, $CDCl_3$, δ):

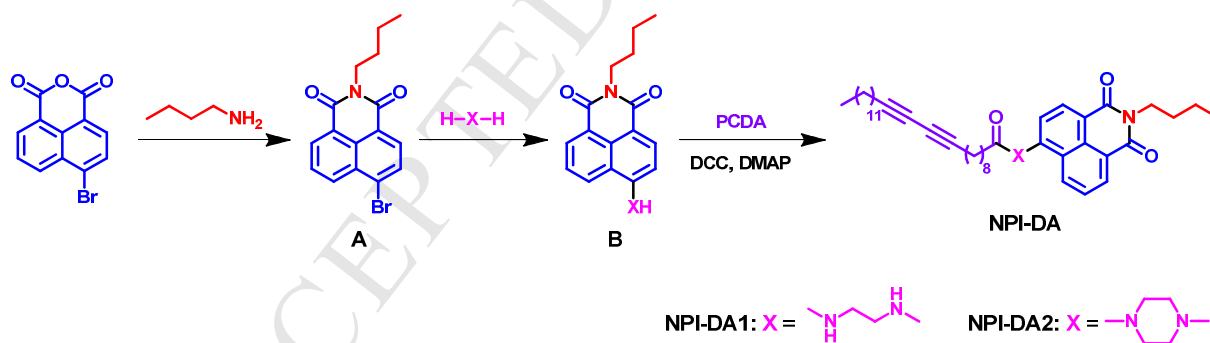
161 171.9, 164.3, 163.9, 155.1, 132.3, 131.2, 129.8, 129.7, 126.3, 126.1, 123.5, 117.7, 115.4, 77.6,

162 77.4, 65.3, 65.2, 53.1, 53.1, 45.8, 41.7, 40.1, 33.3, 31.9, 30.2, 29.6, 29.6, 29.6, 29.4, 29.4, 29.3,

163 29.2, 29.1, 28.9, 28.8, 28.7, 28.3, 28.3, 25.3, 22.7, 20.4, 19.2, 14.1, 13.8. HRMS m/z : $[M + Na]^+$

164 calcd for $C_{45}H_{63}N_3O_3$, 716.4767; found, 716.4767.

165



171 The **NPI-DA** monomer was ground into a fine powder using a mortar and pestle and then
172 polymerized with UV irradiation using a 254 nm lamp for 1 h at room temperature. Finally, a
173 green-colored **NPI-PDA** was collected, and it was used without further purification.

174

175 *2.4. Preparation of the NPI-DA-embedded PEO film*

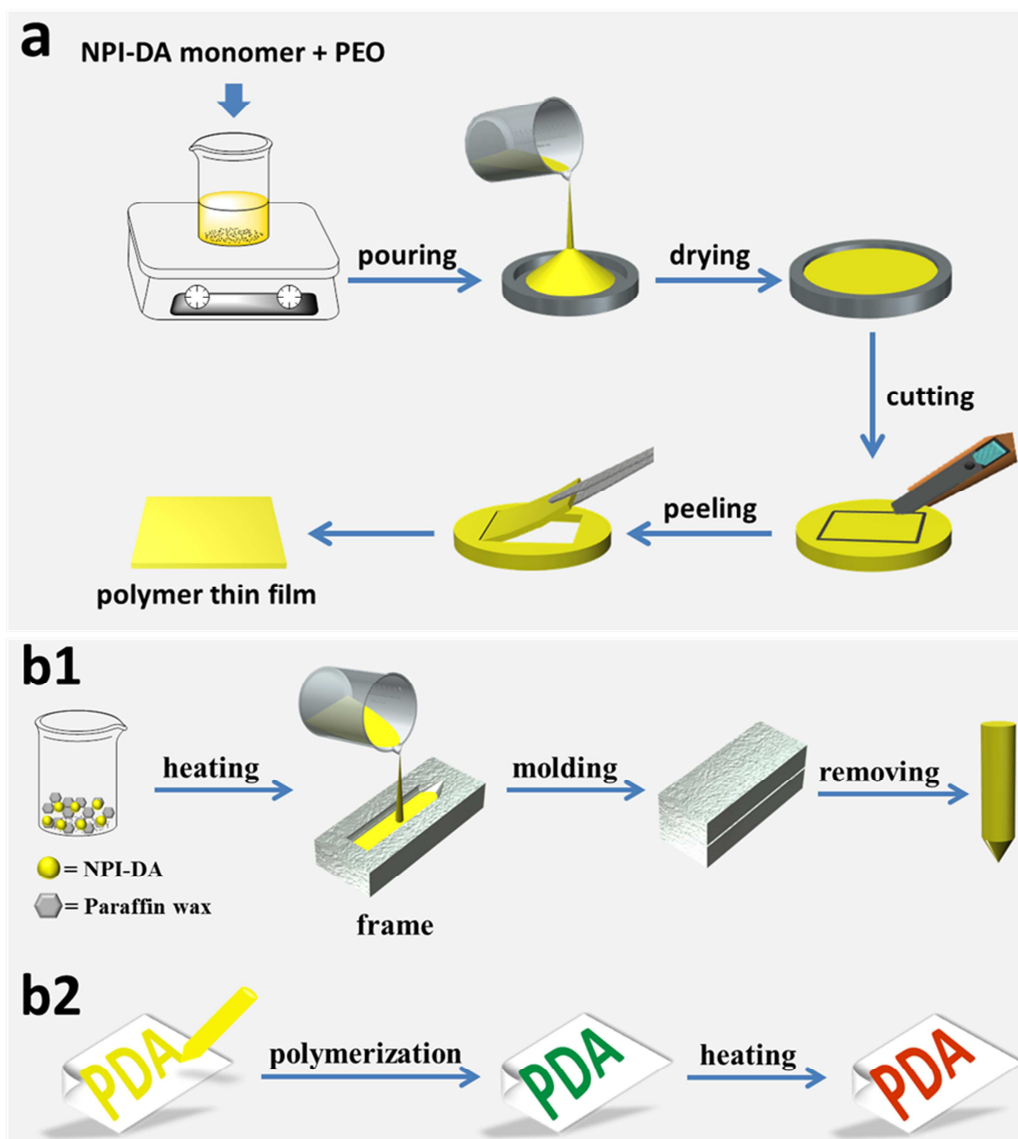
176 Poly(ethylene oxide) was used as the polymer matrix to prepare the polymeric films. As
177 depicted in the schematic representation (**Figure 1**), to the stirred solution of CHCl_3 (3 mL)
178 containing 100 mg of PEO was added 20 mg of **NPI-DA** monomer. After the PEO had
179 completely dissolved, the transparent solution was poured into a petri dish. The solvent was
180 allowed to slowly evaporate under a vacuum dryer for 1 h. The thin PEO films were cut into 2×2
181 cm square pieces and then removed from the petri dish.

182

183 *2.5. Fabrication of an NPI-DA-embedded hand-writable pen*

184 For drawing purposes, a paraffin wax-based hand-writable pen containing **NPI-DA**
185 monomer was constructed. As demonstrated in **Figure 1**, a hot solution of paraffin wax (90%)
186 containing DA monomer (10%) was poured into a mold. After cooling to room temperature, the
187 yellow-colored stick was removed from the mold and could then be used as a thermochromic
188 drawing tool. As shown in the figure, the color transition takes place upon heating a solid surface
189 that has already been drawn with the PDA-wax pen and polymerized.

190



191

192

193 **Figure 1.** (a) Schematic representation of the steps involved in the preparation of polymer thin

194 film. (b1) Fabrication of a diacetylene monomer-embedded paraffin pen. (b2) Color transition of

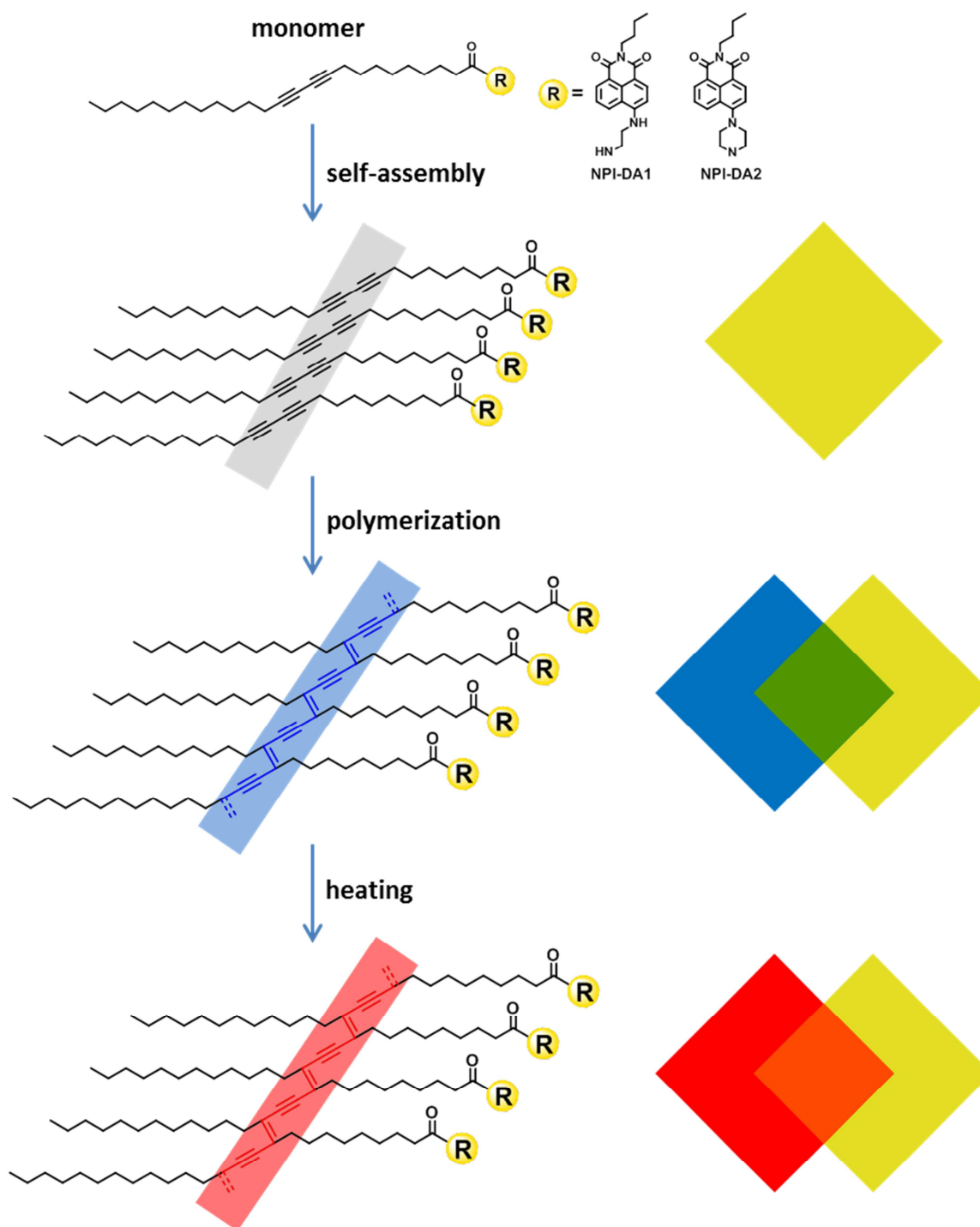
195 the paraffin wax drawing upon polymerization and heating.

196

197 **3. Results and Discussion**

198 *3.1. Thermochromism of green PDAs*

199 Green PDAs were obtained upon polymerization of the diacetylene monomers **NPI-DA1**
200 and **NPI-DA2** under UV light irradiation. To date, the majority of PDAs and their derivatives are
201 blue in color, and this is the first report of using a yellow-colored naphthalimide derivative as a
202 head group to prepare green PDAs. The topochemical polymerization initiated and accelerated
203 by UV irradiation generates the conjugated polymer network [7,8]. To gain a better
204 understanding of the development of green PDA, an illustration showing the self-assembly of the
205 **NPI-DA** monomer, the polymerization and the color transition upon heat treatment is shown in
206 **Figure 2**. As seen in the figure, the monomers approach each other in a single plane upon self-
207 assembly. Under UV irradiation, the adjacent highly ordered monomers join together to produce
208 polymer of **NPI-DA**. The developed green-colored PDAs turns red under thermal stress in the
209 solid state.



210

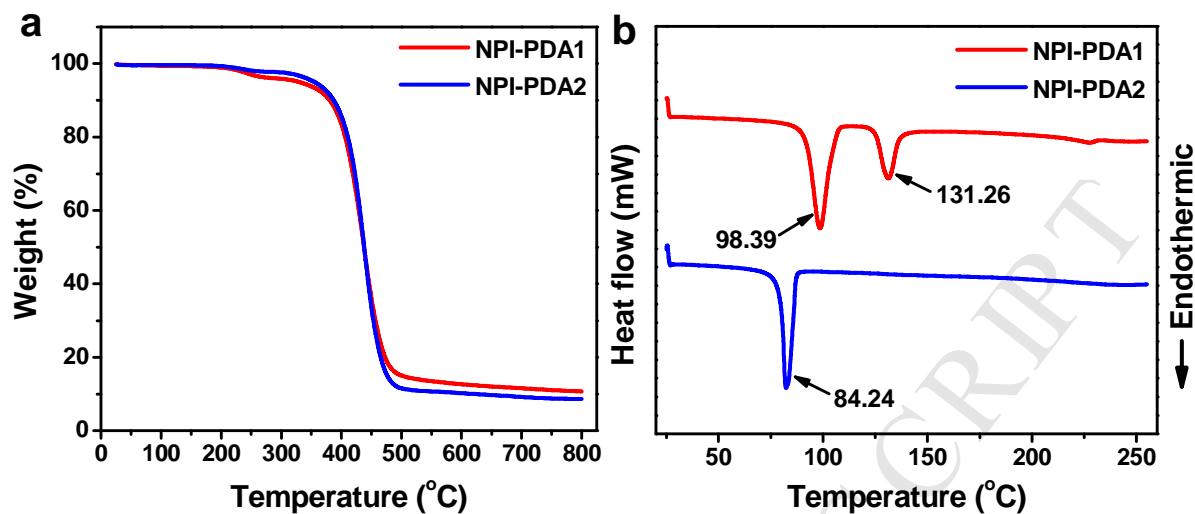
211 **Figure 2.** A detailed schematic illustration of the steps involved in producing a green PDA from
 212 the DA monomer and its thermochromic behavior.

213

214 Initially, the monomers are yellow, and they turn green upon polymerization (see **Figure**
215 **S1** in the SI). UV-vis absorption spectra corresponding to the green and red phases of the PDAs
216 in the powder state were recorded and are shown in (see **Figure S2** in the SI). For the green
217 phase, the most prominent spectral features are two broad peaks centered at approximately 450
218 and 620 nm for **NPI-PDA1** and 400 and 600 nm for **NPI-PDA2**. The PDA undergoes a color
219 transition from green to red when the temperature is increased to 45 °C, and the PDA can be
220 returned to its original green color by decreasing the temperature. The **NPI-PDAs** displayed
221 excellent thermochromic reversibility in the temperature range of 25–160 °C. In the red phase,
222 unexpected absorption shifts were observed due to inadequate polymerization in the powder
223 phase. To avoid this, we then prepared and characterized PEO polymer thin films doped with
224 **NPI-DA** monomer. Additionally, the thin polymer films are clear to the naked-eye and show
225 good spectral properties. Notably, higher temperatures of 180 and 160 °C, which are equal to the
226 melting points of **NPI-PDA1** and **NPI-PDA2**, respectively, will cause irreversible
227 thermochromic behavior in the solid state.

228 To determine the thermal stability of the synthesized PDAs, thermogravimetric analysis
229 (TGA) was conducted over the range of 25–800 °C. As shown in **Figure 3a**, **NPI-PDA1** and
230 **NPI-PDA2** have similar thermal decomposition behavior, and both compounds started
231 decomposing at approximately 350 °C. In the DSC curve of **NPI-PDA1**, two endothermic peaks
232 were observed at 98.39 and 131.26 °C, while **NPI-PDA2** displayed a single endothermic peak at
233 84.24 °C (**Figure 3b**). According to the obtained TGA and DSC data, the prepared PDAs can be
234 analyzed and display their thermochromic properties at reasonably high temperatures.

235



236
 237 **Figure 3.** TGA (a) and DSC (b) curves of **NPI-PDA1** and **NPI-PDA2**. The heating rate was 10
 238 °C/min.

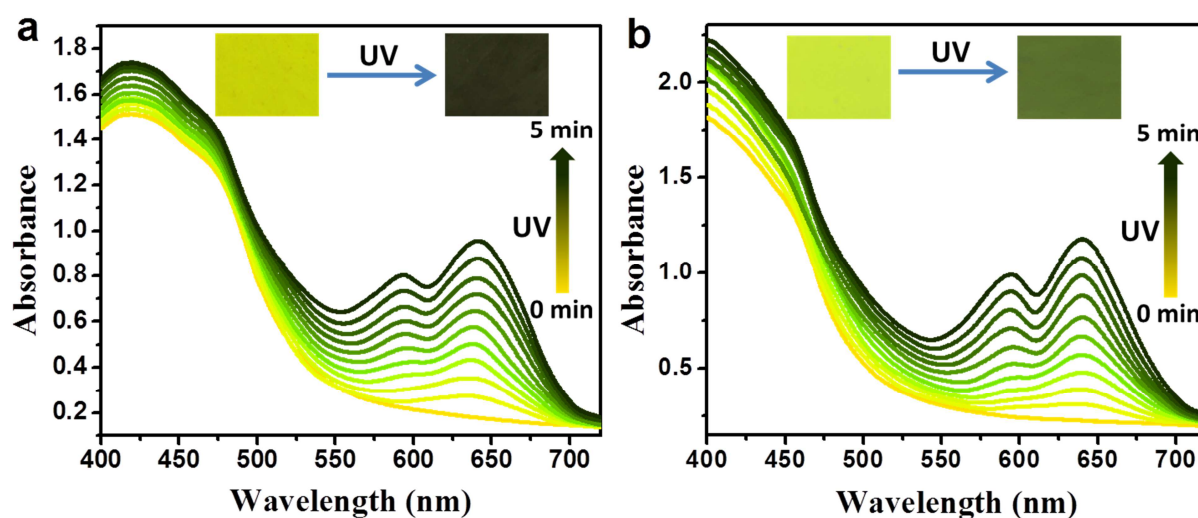
239

240 3.2. Thermochromism of NPI-DA-embedded PEO films

241 Due to its uniformity and the availability of higher surface area to polymerization, we
 242 prepared **NPI-DA**-embedded PEO films. These thin films displayed an extremely quick response
 243 to UV irradiation to yield a green color. The fabricated yellow-colored PEO-based films were
 244 irradiated with a UV lamp (254 nm) at room temperature for 5 min to achieve the polymerized
 245 green-colored films, and the corresponding UV spectra are shown in **Figure 4**. The
 246 naphthalimide moiety connected to ethylenediamine (primary amine) produced brighter green
 247 compared to piperazine (secondary amine) due to the difference in their original yellow colors.
 248 The color of PDA is also depends on the intermolecular hydrogen bonds between two adjacent
 249 polymerizable monomers [60]. Thus, a strong color observed for **NPI-PDA1** could be due to the
 250 formation of strong intermolecular hydrogen bonds that induces the polymerization of
 251 monomers. The **NPI-DA** monomer showed a very broad and more intense peak in the region of
 252 400–500 nm that can be attributed to the naphthalimide chromophore, no peak was observed in

253 the range of 550–700 nm, and a peak centered at 640 nm with a shoulder at approximately 590
254 nm was observed during the polymerization process. In general, a very strong absorption appears
255 at around 650 nm for PDA macromolecules. Instead, a broad absorption peak in the 550–700 nm
256 region was observed, which mainly due to the overlap with the broad and strong absorption band
257 of naphthalimide chromophore. As shown in the spectra, the λ_{max} at approximately 640 nm
258 gradually increased and reached a maximum, and the yellow-colored thin films dramatically
259 turned green after 5 min of UV irradiation. SEM analysis was carried out to observe the
260 morphology of only the thin films of PEO, **NPI-PDA1**-embedded PEO and **NPI-PDA2**-
261 embedded PEO (**Figure 5**). The SEM results of PEO show that the surface is an aggregated
262 sheet. The morphology of the PDA/PEO mixture is completely different, and they show
263 aggregated needles-type morphology. The obtained green PDA-embedded PEO solid film was
264 further heated for the thermochromic observations. The thermochromic transition of the
265 successfully fabricated and polymerized thin films were carried out using photography and
266 electronic absorption spectroscopy.

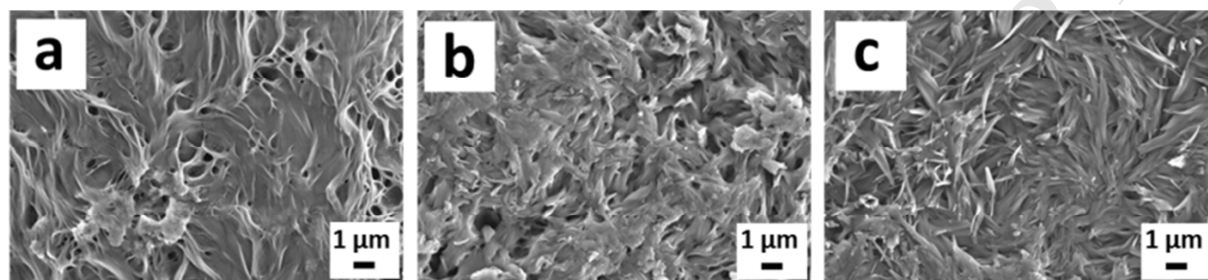
267



268

269 **Figure 4.** UV-vis spectral changes of (a) **NPI-DA1-** and (b) **NPI-DA2-**embedded PEO films
 270 under UV irradiation for 5 min. Inset: The color changes of the thin films from yellow to green
 271 upon polymerization.

272



273

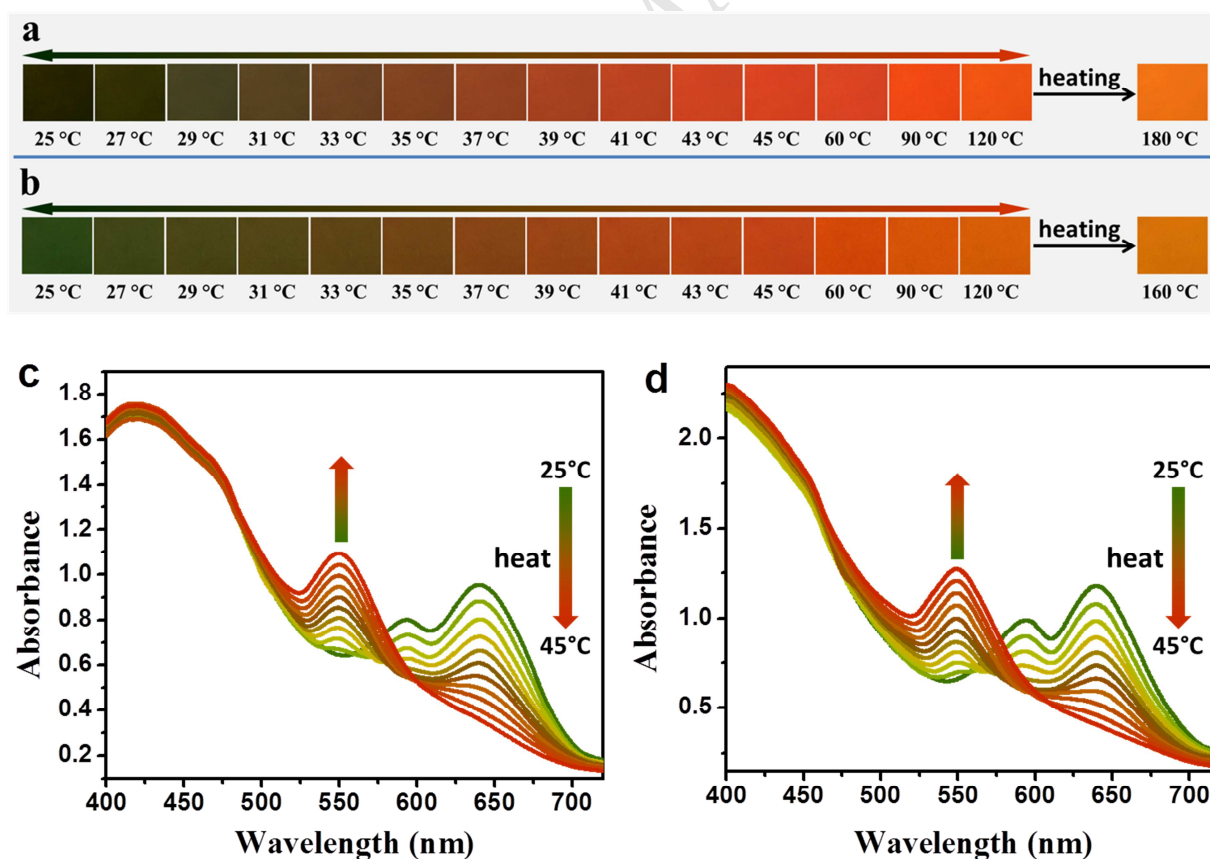
274 **Figure 5.** SEM images of PEO (a), **NPI-PDA1-**embedded PEO (b) and **NPI-PDA2-**embedded
 275 PEO (c) films at room temperature.

276

277 As depicted in **Figure 6**, the reversible significant color transition and the changes in its
 278 absorption spectrum were observed and recorded at 2 °C increments in the temperature range of
 279 25–45 °C. Initially, at 25 °C, the film was green and showed a broad absorption peak centered at
 280 640 nm. The color slowly turned orange-red, and the absorbance at 640 nm gradually decreased,
 281 and a new absorption peak at approximately 550 nm (blueshift) appeared as the temperature
 282 increased. The peak at 640 nm almost disappeared, and the new peak at 550 nm reached its
 283 maximum intensity at 45 °C. The band corresponding to the naphthalimide did not change as the
 284 temperature increase, which means that the naphthalimide group was not affected during
 285 polymerization or heat treatment. The original spectral pattern and color were completely
 286 recovered upon cooling from 45 °C to 25 °C. It is commonly believed that the side chains that
 287 are directly linked to the backbone of the polymer undergo twisting upon thermal treatment. Due
 288 to the presence of twisted side chains, the conjugation within the polymer decreases, causing a

289 blueshift in the absorption spectra [61–63]. On further increasing the temperature from 45–120
290 °C, the orange-red color slowly became orange. The thermochromic reversibility of the PDA-
291 embedded PEO films was successfully demonstrated up to 120 °C. Finally, upon further heat
292 treatment of the orange **NPI-PDA1**- and **NPI-PDA2**-embedded PEO films at 180 and 160 °C,
293 respectively, an irreversible yellow-orange color developed. The thermal stability for PEO films
294 was found to be 180 and 160 °C respectively for **NPI-PDA1** and **NPI-PDA2**. Thus, the PDA in
295 the PEO polymer matrix exhibited a rapid green-to-orange response and a reversible orange-to-
296 green thermochromic transition. The color transition of the PDA in the polymer matrix was the
297 same as that observed in the powder form, and compared to the powder form, it showed
298 promising spectral characteristics when embedded in the polymer matrix.

299

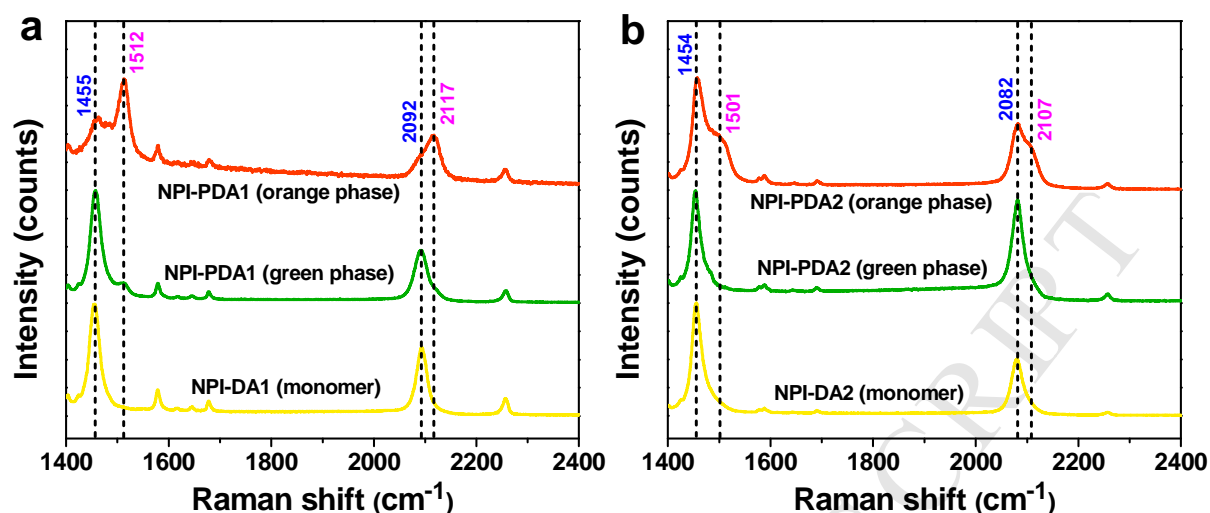


300

301 **Figure 6.** The color transition (a,b) and UV absorption spectral changes (c,d) of polymerized
302 thin films under heating; a and c correspond to **NPI-PDA1**, and b and d correspond to **NPI-**
303 **PDA2**.

304
305 Moreover, the thin films consisting of the monomer and polymer were further
306 characterized using Raman spectrometry. For this study, to generate irreversibly orange films,
307 **NPI-PDA1-** and **NPI-PDA2-**embedded films were heat treated at 180 and 160 °C, respectively.
308 As can be seen in **Figure 7**, peaks corresponding to the alkene and alkyne groups in the **NPI-**
309 **DA1** monomer appeared at 1455 and 2092 cm^{-1} , respectively, and green **NPI-PDA1** showed
310 Raman shifts similar to those of the monomer. The alkene and alkyne bands in the typical orange
311 **NPI-PDA1** appeared at 1512 and 2117 cm^{-1} , respectively, and the bands typical of the initial
312 green polymer were also present. Similarly, the **NPI-DA2** monomer and polymer (green phase)
313 produced signals at 1454 and 2082 cm^{-1} corresponding to the alkene and alkyne groups,
314 respectively. The orange **NPI-PDA2** exhibited the same Raman bands along with shoulder peaks
315 at 1501 and 2107 cm^{-1} . The spectral changes corresponding to the color transition are commonly
316 due to the thermal-induced conformational changes in the alkyl side chains causing changes in
317 the PDA backbone [64–67].

318



319
 320 **Figure 7.** Raman spectral changes of (a) **NPI-DA1**- and (b) **NPI-DA2**-embedded PEO thin films
 321 before and after polymerization (green and orange phase).

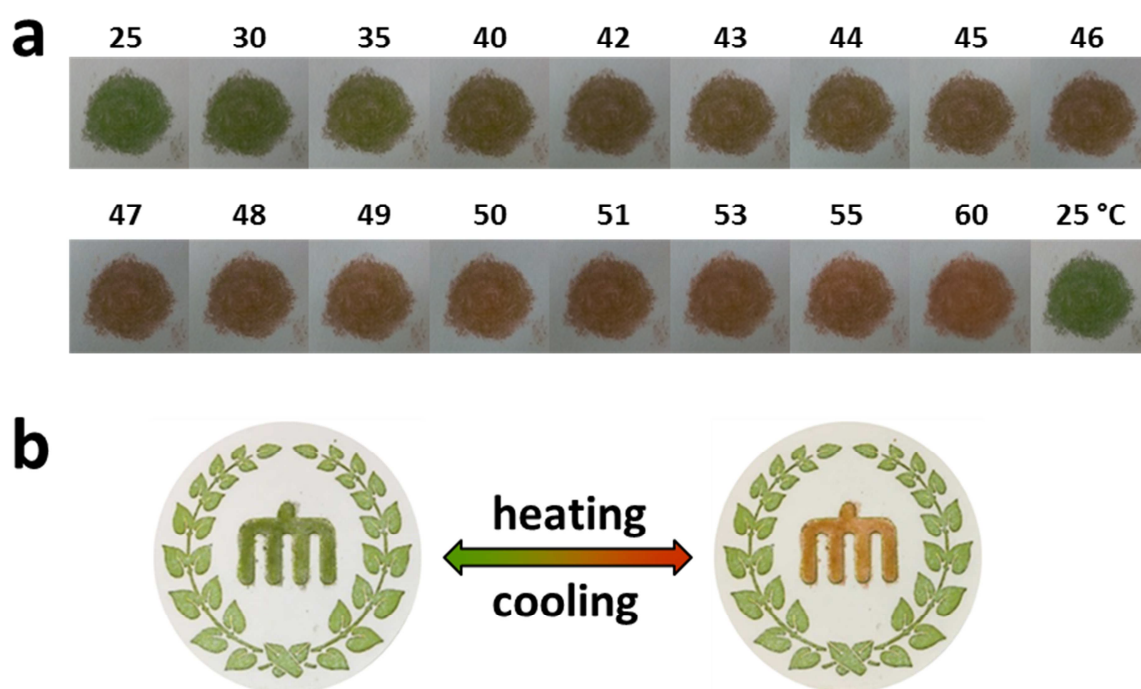
322

323 3.3. Thermochromic properties of NPI-DA-embedded hand-writable pen

324 Due to the unreactive solid matrix, we used crayon wax to fabricate a hand-writable pen
 325 based on the diacetylene monomer and investigated its thermochromic behavior on solid
 326 substrates such as paper. The drawings of **NPI-DA2**-wax crayon on paper showed color changes
 327 upon UV irradiation and thermal treatment, which are photographed step-by-step at various
 328 temperatures (**Figure 8**). As demonstrated in **Figure 9**, images of a parrot and a rose were drawn
 329 using the **NPI-DA1**- and **NPI-DA2**-wax crayons, respectively, and were initially yellow. The
 330 drawings turned green immediately upon UV irradiation (254 nm). The obtained green images
 331 exhibited reversible thermochromic behavior over a wide range of working temperatures from
 332 25–160 °C and 25–180 °C for **NPI-DA1**- and **NPI-DA2**-embedded wax crayons, respectively.
 333 The color of each of the green drawings was monitored over various temperature ranges as
 334 shown in the figure. The images turned greenish-red and orange-red at 35 and 45 °C, and these
 335 color changes are completely reversible. On further heating, the parrot and rose turned orange at

336 180 and 160 °C, respectively, and they returned to green upon cooling. The images
337 corresponding to **NPI-DA1** and **NPI-DA2** irreversibly turned yellow-orange at approximately
338 190 and 170 °C, respectively. The images drawn using crayon pens exhibited similar
339 thermochromic properties as the monomers showed in the powder state. Thus, due to their high
340 thermal stability and immediate thermochromic reversibility, it is possible to utilize in the
341 identification and authentication of documents.

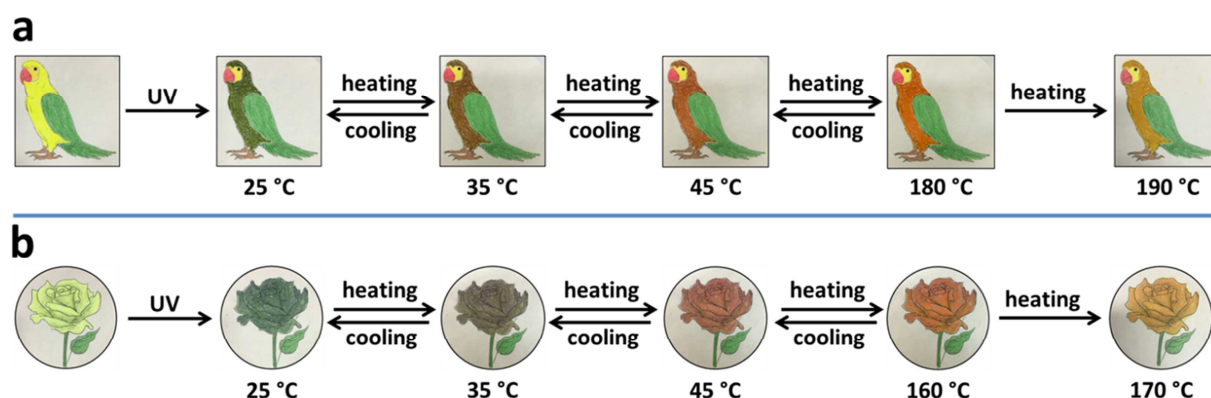
342



343

344 **Figure 8.** Photographs of a PDA image on paper derived from **NPI-PDA2-wax** upon heating and
345 cooling.

346



347

348 **Figure 9.** Photographs of PDA images drawn using the hand-writable pens derived from (a)
 349 **NPI-DA1-** and (b) **NPI-DA2-**wax crayons at various conditions.

350

351 4. Conclusion

352 In the studies described above, the thermochromic behavior of newly synthesized PDAs
 353 was investigated in the solid state as well as in a polymer matrix. PDA-embedded polymer thin
 354 films were fabricated and characterized by SEM, UV absorption and Raman spectroscopic
 355 studies. Obvious spectral changes corresponding to the color transition from green-to-red and
 356 red-to-orange upon heating were observed. Thermochromic reversibility was successfully
 357 monitored in the range of 25–120 °C in the polymer matrix. In addition, **NPI-DA1-** and **NPI-**
 358 **DA2-**embedded paraffin wax-based hand-writable pens were constructed, and they exhibited
 359 excellent reversible thermochromic performance over a wide temperature range (25–160 °C).
 360 Due to their high thermal stability and immediate thermochromic reversibility, these materials
 361 can be used in the identification and authentication of documents.

362

363

364 **Acknowledgements**

365 This study was supported by the Basic Science Research Program through the National Research
366 Foundation of Korea (NRF) funded by the Ministry of Science, ICT and Future Planning (Grant
367 No. NRF-2017R1E1A1A01074266).

368

ACCEPTED MANUSCRIPT

369 **References:**

- 370 [1] Bloor D, Chance RR. Polydiacetylenes: synthesis, structure, and electronic properties.
371 Netherlands: Martinus Nijhoff; 1985.
- 372 [2] Ahn DJ, Chae EH, Lee GS, Shim HY, Chang TE, Ahn KD, Kim JM. Colorimetric
373 reversibility of polydiacetylene supramolecules having enhanced hydrogen-bonding under
374 thermal and pH stimuli. *J Am Chem Soc* 2003;125:8976–7.
- 375 [3] Kim JM, Lee JS, Choi H, Sohn D, Ahn DJ. Rational design and in-situ FTIR analyses of
376 colorimetrically reversible polydiacetylene supramolecules. *Macromolecules* 2005;38:9366–76.
- 377 [4] Park H, Lee JS, Choi H, Ahn DJ, Kim JM. Rational design of supramolecular conjugated
378 polymers displaying unusual colorimetric stability upon thermal stress. *Adv Funct Mater*
379 2007;17:3447–55.
- 380 [5] Beckham GH, Rubner MF. On the origin of thermochromism in cross-polymerized
381 diacetylene-functionalized polyamides. *Macromolecules* 1993;26:5198–201.
- 382 [6] Itoh T, Shichi T, Yui T, Takahashi H, Inui Y, Yakagi KJ. Reversible color changes in lamella
383 hybrids of poly(diacetylenecarboxylates) incorporated in layered double hydroxide nanosheets,
384 *Phys Chem B* 2005;109:3199–206.
- 385 [7] Neabo JR, Tohondjona KIS, Morin J-F. Topochemical polymerization of a diarylbutadiyne
386 derivative in the gel and solid states. *Org Lett* 2011;13:1358–61.
- 387 [8] Matsumoto A, Sada K, Tashiro K, Miyata M, Tsubouchi T, Tanaka T.; Odani, T, Nagahama
388 S, Tanaka T, Inoue K, Saragai S, Nakamoto S. Reaction principles and crystal structure design
389 for the topochemical polymerization of 1,3-dienes. *Angew Chem Int Ed* 2002;41:2502–05.
- 390 [9] Yuan Z, Lee C-W, Lee S-H. Reversible thermochromism in hydrogen-bonded polymers
391 containing polydiacetylenes. *Angew Chem Int Ed* 2004;43:4197–200.

- 392 [10] Yoo K, Kim S, Han N, Kim GE, Shin MJ, Shin JS, Kim M. Stepwise blue-red-yellow color
393 change of a polydiacetylene sensor through internal and external transitions, *Dyes Pigm*
394 2018;149:242–5.
- 395 [11] Okada S, Peng S, Spevak W, Charych D. Color and chromism of polydiacetylene vesicles.
396 *Acc Chem Res* 1998;31:229–39.
- 397 [12] Ahn DJ, Kim JM. Fluorogenic polydiacetylene supramolecules: immobilization,
398 micropatterning, and application to label-free chemosensors. *Acc Chem Res* 2008;41:805–16.
- 399 [13] Yoon J, Chae SK, Kim JM. Colorimetric sensors for volatile organic compounds (VOCs)
400 based on conjugated polymer-embedded electrospun fibers. *J Am Chem Soc* 2007;129:3038–39.
- 401 [14] Nallicheri RA, Rubner MF. Investigations of the mechanochromic behavior of
402 poly(urethane-diacetylene) segmented copolymers. *Macromolecules* 1991;24:517–25.
- 403 [15] Cheng Q, Stevens RC. Charge-induced chromatic transition of amino acid-derivatized
404 polydiacetylene liposomes. *Langmuir* 1998;14:1974–6.
- 405 [16] Jeon H, Lee J, Kim MH, Yoon J. Polydiacetylene-based electrospun fibers for detection of
406 HCl gas. *Macromol Rapid Commun* 2012;33:972–6.
- 407 [17] Ngampeungpis W, Tumcharern G, Pienpinijtham P, Sukwattanasinitt M. Colorimetric UV
408 sensors with tunable sensitivity from diacetylenes. *Dyes Pigm* 2014;101:103–8.
- 409 [18] Charych DH, Nagy JO, Spevak W, Bednarski MD. Direct colorimetric detection of a
410 receptor-ligand interaction by a polymerized bilayer assembly. *Science* 1993;261:585–8.
- 411 [19] Reichert A, Nagy JO, Spevak W, Charych D. Polydiacetylene liposomes functionalized with
412 sialic acid bind and colorimetrically detect influenza virus. *J Am Chem Soc* 1995;117:829–30.

- 413 [20] Kantha C, Kim H, Kim Y, Heo J-M, Joung JF, Park S, Kim J-M. Topochemical
414 polymerization of macrocyclic diacetylene with a naphthalene moiety for a tubular-shaped
415 polydiacetylene chromophore. *Dyes Pigm* 2018;154:199–204.
- 416 [21] Ryu S, Yoo I, Song S, Yoon B, Kim J-M. A thermoresponsive fluorogenic conjugated
417 polymer for a temperature sensor in microfluidic devices. *J Am Chem Soc* 2009;131:3800–1.
- 418 [22] Kwon IK, Song MS, Won SH, Choi SP, Kim M, Sim SJ. Signal amplification by magnetic
419 force on polydiacetylene supramolecules for detection of prostate cancer. *Small* 2012;8:209–13.
- 420 [23] Chen X, Kang S, Kim MJ, Kim J, Kim YS, Kim H, Chi B, Kim S-J, Lee JY, Yoon J. Thin-
421 film formation of imidazolium-based conjugated polydiacetylenes and their application for
422 sensing anionic surfactants. *Angew Chem Int Ed* 2010;49:1422–5.
- 423 [24] Lee J, Jeong EJ, Kim J. Selective and sensitive detection of melamine by intra/inter
424 liposomal interaction of polydiacetylene liposomes. *Chem Commun* 2011;47:358–60.
- 425 [25] Yoo K, Kim S, Han N, Kim GE, Shin MJ, Shin JS, Kim M. Stepwise blue-red-yellow color
426 change of a polydiacetylene sensor through internal and external transitions. *Dyes Pigm*
427 2018;149:242–5.
- 428 [26] Charych DH, Nagy JO, Spevak W, Bednarski MD. Direct colorimetric detection of a
429 receptor-ligand interaction by a polymerized bilayer assembl. *Science* 1993;261:585–8.
- 430 [27] Wang M, Wang F, Wang Y, Zhang W, Chen X. Polydiacetylene-based sensor for highly
431 sensitive and selective Pb^{2+} detection. *Dyes Pigm* 2015;120:307–13.
- 432 [28] Chen X, Yoon J. Thermally reversible temperature sensor based on polydiacetylene:
433 Synthesis and thermochromic properties. *Dyes Pigm* 2011;89:194–8.

- 434 [29] Lee S, Lee J, Lee M, Cho YK, Baek J, Kim J, Park S, Kim MH, Chang R, Yoon J.
435 Construction and molecular understanding of an unprecedented, reversibly thermochromic bis-
436 polydiacetylene. *Adv Funct Mater* 2014; 24:3699-3705.
- 437 [30] Pan JJ, Charych D. Molecular recognition and colorimetric detection of cholera toxin by
438 polymerized liposomes. *Langmuir* 1997;13:1365–7.
- 439 [31] Lifshitz Y, Golan Y, Konovalov O, Berman A. Structural transitions in polydiacetylene
440 langmuir films. *Langmuir* 2009;25:4469–77.
- 441 [32] Okada SY, Jelinek R, Charych D. Induced color change of conjugated polymeric vesicles by
442 interfacial catalysis of phospholipase A2. *Angew Chem Int Ed* 1999;38:655–9.
- 443 [33] Phollookin C, Wacharasindhu S, Ajavakom A, Tumcharern G, Ampornpun S, Eaidkong T,
444 Sukwattanasinitt M. Tuning down of color transition temperature of thermochromically
445 reversible bisdiynamide polydiacetylenes. *Macromolecules* 2010;43:7540–8.
- 446 [34] Morigaki K, Baumgart T, Jonas U, Offenhäusser A, Knoll W. Photopolymerization of
447 diacetylene lipid bilayers and its application to the construction of micropatterned biomimetic
448 membranes. *Langmuir* 2002;18:4082–9.
- 449 [35] Lee S, Kim J-Y, Chen X, Yoon J. Recent progress in stimuli-induced polydiacetylenes for
450 sensing temperature, chemical and biological targets. *Chem Commun* 2016;52:9178–96.
- 451 [36] Rangin M, Basu A. Lipopolysaccharide identification with functionalized polydiacetylene
452 liposome sensors. *J Am Chem Soc* 2004;126:5038–9.
- 453 [37] Wang C, Ma Z. Colorimetric detection of oligonucleotides using a polydiacetylene vesicle
454 sensor. *Anal Bioanal Chem* 2005;382:1708–10.

- 455 [38] Pan X, Wang Y, Jiang H, Zou G, Zhang Q. Benzo-15-crown-5 functionalized
456 polydiacetylene-based colorimetric self-assembled vesicular receptors for lead ion recognition. *J*
457 *Mater Chem* 2011;21:3604–10.
- 458 [39] Swager TM. The molecular wire approach to sensory signal amplification. *Acc Chem Res*
459 1998;31:201–7.
- 460 [40] Kraft A, Grimsdale AC, Holmes AB. Electroluminescent conjugated polymers-seeing
461 polymers in a new light. *Angew Chem Int Ed* 1998;37:402–28.
- 462 [41] Bunz UHF. Poly(aryleneethynylene)s: syntheses, properties, structures, and applications.
463 *Chem Rev* 2000;100:1605–44.
- 464 [42] Maeda K, Yashima E. Dynamic helical structures: detection and amplification of chirality.
465 *Top Curr Chem* 2006;265:47–88.
- 466 [43] Skotheim T A, Reynolds JR. Eds. *Handbook of Conjugating Polymers*. 3rd ed. New York:
467 CRC Press; 2007.
- 468 [44] Dimitrakopoulos CD, Malenfant PRL. Organic thin film transistors for large area
469 electronics. *Adv Mater* 2002;14:99–117.
- 470 [45] Dong W, Lin G, Wang H, Lu W. New dendritic polydiacetylene sensor with good reversible
471 thermochromic ability in aqueous solution and solid film. *ACS Appl Mater Interfaces*
472 2017;9:11918–23.
- 473 [46] Yang P-C, Wang Y-H, Wu H. Synthesis, characterization, and photochemical properties of
474 chromophores containing photoresponsive azobenzene and stilbene. *J Appl Polym Sci*
475 2012;124:4193–05.

- 476 [47] Chen X, Hong L, You X, Wang Y, Zou G, Su W, Zhang Q. Photo-controlled molecular
477 recognition of α -cyclodextrin with azobenzene containing polydiacetylene vesicles. *Chem*
478 *Commun* 2009;1356–8.
- 479 [48] Ye Q, You X, Zou G, Yu X, Zhang Q. Morphology, structure and chromatic properties of
480 azobenzene-substituted polydiacetylene supramolelular assemblies. *J Mater Chem*
481 2008;18:2775–80.
- 482 [49] Wang Y, Chen X, Zou G, Zhang Q. Molecular structure modulated organization and
483 properties of azobenzene-substituted polydiacetylene assemblies films: photopolymerization,
484 morphology, and thermal stability. *Macromol Chem Phys* 2010;211:888–96.
- 485 [50] Kim MJ, Angupillai S, Min K, Ramalingam M, Son Y-A. Tuning of the topochemical
486 polymerization of diacetylenes based on an odd/even effect of the peripheral alkyl chain:
487 thermochromic reversibility in a thin film and a single-component ink for a fountain pen. *ACS*
488 *Appl Mater Interfaces* 2018;10:24767–75.
- 489 [51] Kang B, Min H, Seo U, Lee J, Park N, Cho K, Lee HS. Directly drawn organic transistors
490 by capillary pen: a new facile patterning method using capillary action for soluble organic
491 materials. *Adv Mater* 2013;25:4117–22.
- 492 [52] Lee WH, Min H, Park N, Lee J, Seo E, Kang B, Cho K, Lee HS. Microstructural control
493 over soluble pentacene deposited by capillary pen printing for organic electronics. *ACS Appl*
494 *Mater Interfaces* 2013;5:7838–44.
- 495 [53] Jia H, Wang J, Zhang X, Wang Y. Pen-writing polypyrrole arrays on paper for versatile
496 cheap sensors. *ACS Macro Lett* 2014;3:86–90.
- 497 [54] Russo A, Ahn BY, Adams JJ, Duoss EB, Bernhard JT, Lewis JA. Pen-on-paper flexible
498 electronics. *Adv Mater* 2011;23:3426–30.

- 499 [55] Polavarapu L, Porta AL, Novikov SM, Coronado-Puchau M, Liz-Marzan LM. Pen-on-paper
500 approach toward the design of universal surface enhanced raman scattering substrates. *Small*
501 2014;10:3065–71.
- 502 [56] Mirica KA, Weis JG, Schnorr JM, Esser B, Swager TM. Mechanical drawing of gas sensors
503 on paper. *Angew Chem Int Ed* 2012;51:10740–5.
- 504 [57] Hu L, Choi JW, Yang Y, Jeong S, Mantia FL, Cui L-F, Cui Y Highly conductive paper for
505 energy-storage devices. *Proc Natl Acad Sci USA* 2009;106:21490–4.
- 506 [58] Chae S, Lee JP, Kim JM. Mechanically drawable thermochromic and
507 mechanothermochromic polydiacetylene sensors. *Adv Funct Mater* 2016;26:1769.
- 508 [59] Kim M, Mergu N, Son Y-A. Imidazole-containing ratiometric receptor for the selective and
509 sensitive detection of cyanide and fluoride via deprotonation and a receptor-anion ensemble for
510 Cu^{2+} sensing. *J Lumin* 2018;204:244–252.
- 511 [60] Ampornpun S, Montha S, Tumcharern G, Vchirawongkwin V, Sukwattanasinitt M,
512 Wacharasindhu S. Odd–even and hydrophobicity effects of diacetylene alkyl chains on
513 thermochromic reversibility of symmetrical and unsymmetrical diyndiamide polydiacetylenes.
514 *Macromolecules* 2012;45:9038–45.
- 515 [61] Pang J, Yang L, McCaughey BF, Peng H, Ashbaugh HS, Brinker CJ, Lu Y.
516 Thermochromatism and structural evolution of metastable polydiacetylenic crystals. *J Phys*
517 *Chem B* 2006;110:7221–5.
- 518 [62] Nie X, Wang G. Synthesis and self-assembling properties of diacetylene-containing
519 glycolipids. *J Org Chem* 2006;71:4734–41.
- 520 [63] Lee D-C, Sahoo SK, Cholli AL, Sandman DJ. Structural aspects of the thermochromic
521 transition in urethane-substituted polydiacetylenes. *Macromolecules* 2002;35:4347–55.

- 522 [64] Park IS, Park HJ, Jeong W, Nam J, Kang Y, Shin K, Chung H, Kim J-M. Low temperature
523 thermochromic polydiacetylenes: design, colorimetric properties, and nanofiber formation.
524 *Macromolecules* 2016;49:1270–8.
- 525 [65] Kim D-Y, Lee S-A, Jung D, Jeong K-U. Photochemical isomerization and topochemical
526 polymerization of the programmed asymmetric amphiphiles. *Sci Rep* 2016;6:28659.
- 527 [66] Chen C, Chen J, Wang T, Liu M. Fabrication of helical nanoribbon polydiacetylene via
528 supramolecular gelation: circularly polarized luminescence and novel diagnostic chiroptical
529 signals for sensing. *ACS Appl Mater Interfaces* 2016;8:30608–15.
- 530 [67] Huo J, Deng Q, Fan T, He G, Hu X, Hong X, Chen H, Luo S, Wang Z, Chen D. Advances
531 in polydiacetylene development for the design of side chain groups in smart material applications
532 -a mini review. *Polym Chem* 2017;8:7438–45.

Highlights

- Novel PDAs show reversible green-to-red colorimetric transition upon heating.
- PEO films are fabricated and characterized by SEM, UV and Raman spectroscopy.
- Crayon hand-writable pens are fabricated and used efficiently on a solid substrate.
- PDAs work efficiently and reversibly in the ranges of 25–120 °C and 25–160 °C.